

Article

# Synthesis and Investigation of Novel Optical Active SiO<sub>2</sub> glasses with entrapped YAG:Ce synthesized by sol-gel method

Monika Skruodiene <sup>1,\*</sup>, Meldra Kemere <sup>1</sup>, Greta Inkrataite <sup>2</sup>, Madara Leimane <sup>1</sup>, Rimantas Ramanauskas <sup>3</sup>, Ramunas Skaudzius <sup>2</sup> and Anatolijs Sarakovskis <sup>1</sup>

<sup>1</sup> Institute of Solid State Physics, University of Latvia, 8 Kengaraga str., LV-1063 Riga, Latvia;

<sup>2</sup> Institute of Chemistry, Faculty of Chemistry and Geosciences, Vilnius University, Naugarduko 24, LT-03225, Vilnius, Lithuania;

<sup>3</sup> State research institute Center for Physical Sciences and Technology, Saulėtekio av. 3, LT-10257 Vilnius, Lithuania.

\* Correspondence: monika.skruodiene@cfi.lu.lv; Tel.: +370 6 25 68856

**Abstract:** We present a crack-free optically active SiO<sub>2</sub> glass-composite material containing YAG:Ce synthesized by a modified sol-gel technique. A glass-composite material consisting of yttrium aluminum garnet doped with Ce<sup>3+</sup> (YAG:Ce) entrapped into a SiO<sub>2</sub> xerogel. This composite material has been prepared by sol-gel technique with modified gelation and drying process to obtain crack-free optically active SiO<sub>2</sub> glass. The concentration of the YAG:Ce was from 0.5 to 2.0 wt%. All synthesized samples were characterized by X-ray diffraction (XRD) and scanning electron microscope (SEM) techniques. The luminescence properties of the obtained materials were studied.

**Keywords:** optical active; luminescence; sol-gel; synthesis; YAG:Ce; SiO<sub>2</sub>; glass.

## 1. Introduction

Sol-gel techniques for a long time have been used for the fabrication of glasses and ceramics. Sol-gel synthesis is a widely used method for the preparation of glasses. This method involves the creation of a sol, which converts into a gel and then a glass upon thermal treatment. The sol-gel process can produce glasses with various compositions and structures, making it a versatile and flexible technique. One of the advantages of sol-gel synthesis for glass production is the ability to create complex systems with high surface areas and uniform morphology. The process allows for precise particle size and shape control and consistent glass properties and performance. In addition to offering a cost-effective and scalable approach to glass production, sol-gel synthesis is a sustainable method with a low cost and environmental impact [1–5].

The sol-gel technique of preparing glasses is still being studied. Glasses synthesized by the sol-gel method have attracted much interest because of the possibility of synthesizing glass components, for example, optical fibers, lenses, mirrors, etc. Optically active SiO<sub>2</sub> glasses are a fascinating class of materials due to their interesting optical properties and potential applications in various fields. A small amount of dopant ions causes the optical activity of SiO<sub>2</sub> glasses. Optically active SiO<sub>2</sub> glasses have several potential applications in optics and photonics. For example, they can be used in polarization-sensitive optical devices, such as polarizers, waveplates, and optical rotators. They can also be used in sensing applications, where changes in optical activity can be used to detect chemical or biological molecules. Optically active SiO<sub>2</sub> glasses represent a fascinating and rapidly evolving field of research with significant potential applications in optics, photonics, sensing, and fundamental science. SiO<sub>2</sub> glasses have proven helpful as host materials for rare-earth ions in solid-state lasers. For several practical reasons, glasses doped with Nd<sup>3+</sup> have found the most comprehensive application. Among other rare-earth-containing materials, Er<sup>3+</sup>-doped glasses are currently generating much interest as fiber amplifiers in optical communications systems [6–9].

White LED technology is based on blue LED chips, first developed by Nichia Co. in 1991. These chips are coated with yellow emitting phosphor to create white light. One popular phosphor used for this purpose is  $\text{Ce}^{3+}$  doped YAG phosphor. This phosphor has been available since the 1960s, but it is considered a cool-light phosphor due to the lack of a red component in its emission spectrum. To shift its emission spectrum by substituting the  $\text{Y}^{3+}$  or  $\text{Al}^{3+}$  with different ions. For example, replacing  $\text{Y}^{3+}$  with rare-earth ions like  $\text{Tb}^{3+}$ ,  $\text{Gd}^{3+}$ ,  $\text{Dy}^{3+}$ ,  $\text{La}^{3+}$ , etc. can introduce a red-shift, while substituting  $\text{Al}^{3+}$  with ions like  $\text{Ga}^{3+}$  or  $\text{In}^{3+}$  can cause a blue shift in the cerium emission. Co-doping with ions like  $\text{Pr}^{3+}$  can also introduce a secondary peak in the red spectral range. By co-doping a YAG:Ce phosphor with rare earth ions, white LEDs with improved optical properties can be developed. Moreover, adjusting the  $\text{Ce}^{3+}$  concentration or modifying the process parameters can introduce a slight red shift in the emission spectrum. All this research has led to the development of highly efficient and versatile white LED technology [10–15].

## 2. Results and Discussion

### 2.1. X-ray diffraction

The synthesized samples were analyzed by XRD analysis to determine their composition and purity. All peaks were identified. All reflexes were assigned to the garnet phase (YAG COD ID #1529037). The  $\text{SiO}_2$  was not attributed to any diffraction pattern peaks because it is amorphous. Worthy to note that there are no shifts observed in the XRD data, which means that no changes were made during the annealing to the pure garnet crystal phase. It can be stated that YAG:Ce@ $\text{SiO}_2$  composite samples are pure. The XRD patterns of the YAG:0.5%Ce@ $\text{SiO}_2$  composite and YAG:0.5%Ce are presented in Figure 1.

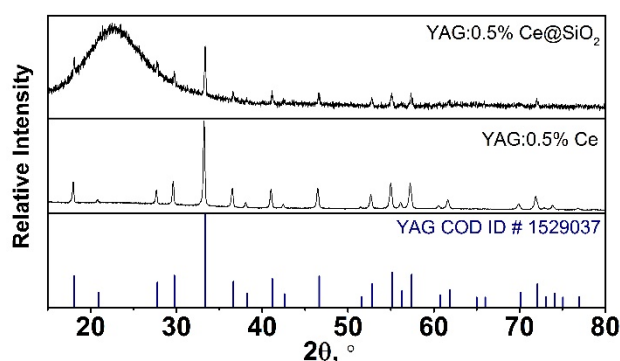


**Figure 1.** XRD patterns of the 0.5%YAG:0.5%Ce@ $\text{SiO}_2$  composite and YAG:0.5%Ce.

### 2.2. Scanning electron microscopy (SEM) analysis

SEM analysis was performed to determine the surface morphology of the synthesized composites. The characterized sample surface is smooth with microcracks. In most of the microcracks, garnet nanoparticles are visible. The majority of the particles are in the size range between 200 to 700 nm. SEM images are presented in Figure 2.

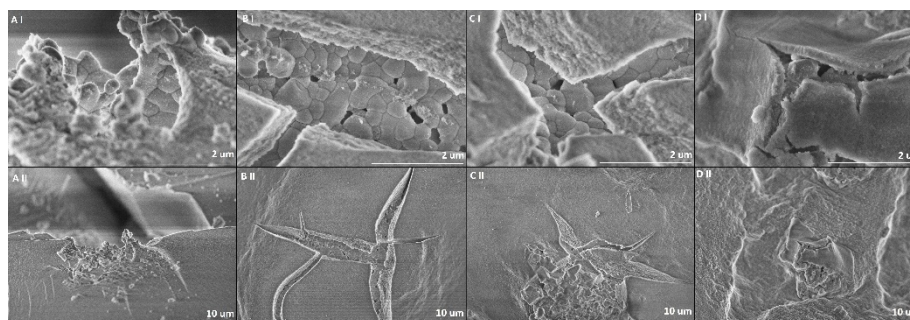


**Figure 2.** SEM images of the samples in different magnifications. 0.5%YAG:0.5%Ce@ $\text{SiO}_2$  (A I,II), 1.0%YAG:0.5%Ce@ $\text{SiO}_2$  (B I,II), 1.5%YAG:0.5%Ce@ $\text{SiO}_2$  (C I,II) and 2.0%YAG:0.5%Ce@ $\text{SiO}_2$  (D I,II)

### 2.3. Luminescence properties

The emission spectra of synthesized samples excited at 458 nm are depicted in Figure 3. In emission spectra, all samples have a wide band with a peak wavelength ( $\lambda_{\max}=538$  nm), which is attributed to the  $[\text{Xe}]5d^1 \rightarrow [\text{Xe}]4f^1$  electron transitions. Increasing the concentration of YAG:0.5%Ce leads to increasing the emission intensity (Fig.3A). This may be due to an increase in the number of optically active centers in the samples as the concentration increases. Normalized luminescence spectra of YAG:0.5%Ce doped samples are shown (Fig.3B). The spectra exhibit a broad band from around 460 nm to 750 nm with the maximal intensity at about 538 nm. Need to note that the spectrum of the 0.5%YAG:0.5%Ce@SiO<sub>2</sub> sample is slightly shifted to the shorter emission wavelength. It could be described as coupling the  $5d$  levels with the surrounding crystal field [14,16–19].

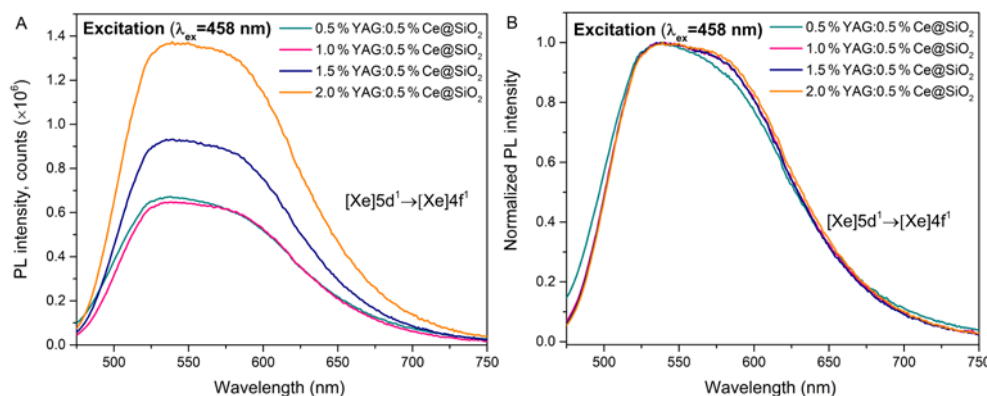


**Figure 3.** Photoluminescence emission spectra of the samples. Emission spectra of 0.5%YAG:0.5%Ce@SiO<sub>2</sub>, 1.0%YAG:0.5%Ce@SiO<sub>2</sub>, 1.5%YAG:0.5%Ce@SiO<sub>2</sub> and 2.0%YAG:0.5%Ce@SiO<sub>2</sub> (A), normalized emission spectra of 0.5%YAG:0.5%Ce@SiO<sub>2</sub>, 1.0%YAG:0.5%Ce@SiO<sub>2</sub>, 1.5%YAG:0.5%Ce@SiO<sub>2</sub> and 2.0%YAG:0.5%Ce@SiO<sub>2</sub> (B).

The photoluminescence quantum yield (PLQY) was calculated. The quantum yield of the analyzed samples is shown in Table 1. The highest luminescence quantum yield value (23 %) was observed in the samples doped with 1.5 % YAG:0.5%Ce and 2 % YAG:0.5%Ce. For other samples, it was lower.

**Table 1.** The quantum yield of the analyzed glass samples.

Sample name	PLQY (%)
0.5%YAG:0.5%Ce@SiO <sub>2</sub>	6 ± 0.5
1.0%YAG:0.5%Ce@SiO <sub>2</sub>	12 ± 1
1.5%YAG:0.5%Ce@SiO <sub>2</sub>	23 ± 2
2.0%YAG:0.5%Ce@SiO <sub>2</sub>	23 ± 2

Another essential analysis for optically active glasses is also the decay time measurements. Luminescence properties were further investigated by measuring the photoluminescence decay curves of the synthesized samples. All the analyzed samples exhibit bi-exponential photoluminescence decay. In Fig. 4C, luminescence decay kinetics with 342 nm are shown. The luminescence decay of samples doped with 1–2 % YAG:0.5%Ce exhibit similar properties while in a sample with 0.5 % YAG:0.5%Ce, the luminescence intensity decreases faster. It could be related to the relative decrease of the green 550 nm luminescence band in the 0.5 % YAG:0.5%Ce doped sample (Fig.4B). All the decay curves were calculated and approximated with a double exponential function:  $A_1$  and  $A_2$  are the fitting parameters,  $\tau_1$ , and  $\tau_2$  are decay times of the fast and slow decay components. Using  $\tau_1$  and  $\tau_2$ , the average lifetime was calculated using the formula:

$$\langle \tau \rangle = \frac{A_1 \tau_1^2 + A_2 \tau_2^2}{A_1 \tau_1 + A_2 \tau_2} \quad (1)$$

The calculated average lifetimes are shown in Table 2. Increasing the concentration of the YAG:0.5%Ce, the decay time increases. The decay times with the higher concentration are very close to the literature (~60 ns) [20].

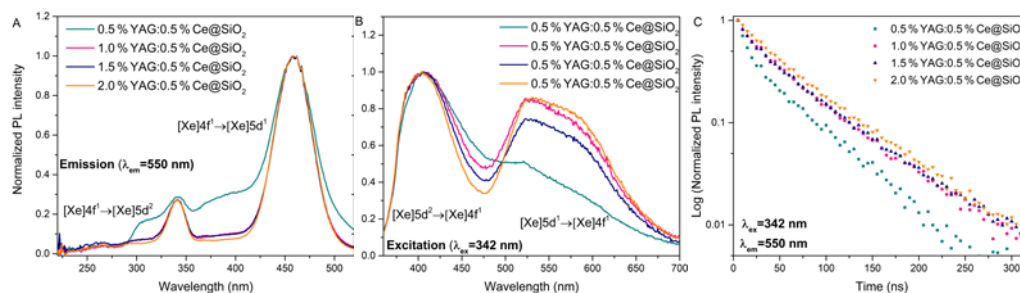


**Figure 4.** Photoluminescence excitation (A), emission (B) spectra, and decay curves (C) of glass samples.

**Table 2.** The calculated luminescence lifetimes and energy transfer efficiency of Ce<sup>3+</sup> ions in glass samples.

Sample name	$\tau$ (ns) $\pm$ 3 ns ( $\lambda_{ex}=342$ nm, $\lambda_{em}=550$ nm)
0.5%YAG:0.5%Ce@SiO <sub>2</sub>	48
1.0%YAG:0.5%Ce@SiO <sub>2</sub>	53
1.5%YAG:0.5%Ce@SiO <sub>2</sub>	57
2.0%YAG:0.5%Ce@SiO <sub>2</sub>	60

### 3. Conclusions

In this study, all single phase YAG:0.5%Ce, synthesized via sol-gel route, garnets were successfully entrapped into SiO<sub>2</sub> glass. YAG:0.5%Ce@ SiO<sub>2</sub> xerogel samples were formed with modified gelation and drying to obtain crack-free glass at relatively low temperatures. It was demonstrated that incorporation does not affect the morphology of the analyzed samples. Glass samples contain microcracks with well-shaped irregular sphere-like particles with size from 200 to 700 nm. Analyzed glass samples were excited at 458 nm. It showed that increasing the concentration of YAG:0.5%Ce leads to increasing the emission intensity. The photoluminescence quantum yield (PLQY) was calculated. The highest luminescence quantum yield value (23 %) was observed in samples with higher concentrations on YAG:0.5%Ce. Furthermore, by increasing the concentration of the YAG:0.5%Ce, the decay time increases (2.0%YAG:0.5%Ce@SiO<sub>2</sub> decay time – 60 ns). The aforementioned optical properties indicate that analyzed optically active glasses can be promising candidates for scintillators and white light-emitting diodes.

### 4. Materials and Methods

#### 4.1. YAG:Ce synthesis procedure via sol-gel route.

For synthesized compounds were used precursors: Y<sub>2</sub>O<sub>3</sub>, Al(NO<sub>3</sub>)<sub>3</sub>·9H<sub>2</sub>O, (NH<sub>4</sub>)<sub>2</sub>Ce(NO<sub>3</sub>)<sub>6</sub> and H<sub>3</sub>BO<sub>3</sub>. Firstly, Y<sub>2</sub>O<sub>3</sub> was dissolved in a concentrated nitric acid at 80 °C. After that, nitric acid was evaporated, and the resulting solution was washed with distilled water three times. Every time water was added, the excess water must be evaporated. After washing with distilled H<sub>2</sub>O, 200 ml of distilled water was added. Then other precursors (Al(NO<sub>3</sub>)<sub>3</sub>·9H<sub>2</sub>O, (NH<sub>4</sub>)<sub>2</sub>Ce(NO<sub>3</sub>)<sub>6</sub>, H<sub>3</sub>BO<sub>3</sub>) were dissolved in the resulting solution. The solution was left to stir on a magnetic stirrer for 2 hours at about 50 °C. After 2 hours, citric acid is added to the solution in a 1:1 ratio of metal ions and left to stir overnight. Finally, the water evaporated at the same temperature. The resulting gel is dried at a temperature of 400 °C for 24 hours. The synthesized xerogel was first heated in air for 2 hours at 1000 °C with 5°/min heating rate, then also was calcinated in air for 4 hours at 1200 °C with 5°/min heating rate.

#### 4.2. YAG:Ce@SiO<sub>2</sub> synthesis procedure via sol-gel route.

The samples were synthesized using the sol-gel method following the procedure described by Kajihara [21] with modified gelation and drying process to obtain crack-free glass. The first step consists of a hydrolysis reaction at room temperature between silicon (Si) organic precursor tetraethoxysilane (TEOS) and deionized water, to which a small amount of nitric acid (HNO<sub>3</sub>) and a certain amount of YAG:Ce. The mixture was then stirred for one hour at room temperature to make

a homogeneous solution. The molar ratio of TEOS:H<sub>2</sub>O:HNO<sub>3</sub> was 1: 22: 0.002. The sol was with pH value between 1 – 2. Then ammonium acetate (AcONH<sub>4</sub>) buffer solution in deionized H<sub>2</sub>O was added to the prepared sol to increase pH value to ~5 – 6 and stirred for additional 2 minutes at room temperature. Prepared sols were then immediately transferred to the container for drying and left for 30 min in the ultrasonic bath to avoid further gel cracking.

Furthermore, the hydrogel was aged slowly in a drying oven starting from room temperature and gradually increasing temperature to 70 °C. The entire drying process took 168 hours. The YAG:Ce@SiO<sub>2</sub> xerogel samples were further used for the post-treatment process at 1000 °C temperature. A xerogel was placed in a quartz tube, heated at a rate of 5 °/min up to the predetermined temperature, and maintained for two hours. Then, translucent YAG:Ce@SiO<sub>2</sub> glass was obtained.

#### 4.3. Characterization.

For phase identification at room temperature the XRD data were collected in 15° – 80° 2θ range (step width of 0.01 °, scan speed 10 °/min, dwell time 5.0 s) using Ni-filtered Cu Kα1 radiation on Rigaku MiniFlexII diffractometer. The measurement current and voltage were set to 15 mA and 30 kV, respectively.

Scanning electron microscopy (SEM) micrographs were taken using Hitachi SU-70 SEM. Powder was fixed on a carbon film. The proper magnification was selected, and images were recorded. The particle size measurements were done using open-source Fiji (ImageJ) software by accidentally selecting random particles.

Photoluminescence emission and excitation spectra were recorded at room temperature using a spectrometer from Edinburgh Instruments (model: FLS1000-DD-stm) equipped with a CW 450 W Xenon lamp (model: Xe2) and a cooled red photomultiplier tube (model: R928P) for detection. The spectra were corrected for the instrumental response. Photoluminescence decay kinetics were recorded using a pulsed tunable nanosecond Nd:YAG laser NT 342/3UV from Ekspla. An Andor Technologies spectrometer SR-303i-B and a time-resolved CCD camera DH734-18F-A3 were employed to record photoluminescence decay curves at room temperature.

**Author Contributions:** For research articles with several authors, a short paragraph specifying their individual contributions must be provided. The following statements should be used “Conceptualization, M. Skruodiene and A. Sarakovskis; methodology, M. Skruodiene, M. Leimane and G. Inkrataite; software, M. Skruodiene; validation, A. Sarakovskis; formal analysis, M. Skruodiene and M. Kemere; investigation, M. Skruodiene; resources, A. Sarakovskis, R. Ramanauskas and R. Skaudzius; data curation, M. Skruodiene; writing—original draft preparation, M. Skruodiene; writing—review and editing, A. Sarakovskis; visualization, M. Skruodiene and M. Kemere; supervision, A. Sarakovskis; project administration, M. Skruodiene. All authors have read and agreed to the published version of the manuscript.” Please turn to the [CRediT taxonomy](#) for the term explanation. Authorship must be limited to those who have contributed substantially to the work reported.

**Data Availability Statement:** The data presented in this study are available in [Synthesis and Investigation of Novel Optical Active SiO<sub>2</sub> glasses with entrapped YAG:Ce synthesized by sol-gel method].

**Acknowledgments:** The work of Monika Skruodiene is supported by ERDF PostDoc project No.1.1.1.2/VIAA/3/19/480.

Institute of Solid State Physics, University of Latvia has received funding from the European Union’s Horizon 2020 Framework Programme H2020-WIDESPREAD-01-2016-2017-TeamingPhase2 under grant agreement No. 739508, project CAMART<sup>2</sup>.

**Conflicts of Interest:** The authors declare no conflict of interest.

## References

1. Zarzycki, J. *Past and Present of Sol-Gel Science and Technology*; Kluwer Academic Publishers, 1996; Vol. 11;.
2. Grandi, S.; Mustarelli, P.; Agnello, S.; Cannas, M.; Cannizzo, A. Sol-Gel GeO<sub>2</sub>-Doped SiO<sub>2</sub> Glasses for Optical Applications. *J. Sol-Gel Sci. Technol.* **2003**, *26*, 915–918.
3. Xia, G.; Zhou, S.; Zhang, J.; Xu, J. Structural and Optical Properties of YAG:Ce<sup>3+</sup> Phosphors by Sol-Gel Combustion Method. *J. Cryst. Growth* **2005**, doi:10.1016/j.jcrysgro.2005.01.072.
4. Inkrataite, G.; Kemere, M.; Sarakovskis, A.; Skaudzius, R. Influence of Boron on the Essential Properties for New Generation Scintillators. *J. Alloys Compd.* **2021**, *875*, doi:10.1016/j.jallcom.2021.160002.

5. Pan, Y.X.; Wang, W.; Liu, G.K.; Skanthakumar, S.; Rosenberg, R.A.; Guo, X.Z.; Li, K.K. Correlation between Structure Variation and Luminescence Red Shift in YAG:Ce. *J. Alloys Compd.* **2009**, *488*, 638–642, doi:10.1016/j.jallcom.2009.04.082.
6. McGahay, V.; Tomozawa, M. *Phase Separation in Rare-Earth-Doped SiO<sub>2</sub> Glasses*; 1993;
7. Continenza, M.A.; Crescente, G.; Pacifico, S.; Catauro, M. Biocompatibility of New SiO<sub>2</sub> Anti-Bacterial Material Synthesized by Sol–Gel Route. *Macromol. Symp.* **2021**, *396*, 2–4, doi:10.1002/masy.202000202.
8. Pawlik, N.; Szpikowska-sroka, B.; Goryczka, T.; Pietrasik, E.; Pisarski, W.A. Luminescence of SiO<sub>2</sub>-BaF<sub>2</sub>:Tb<sup>3+</sup>, Eu<sup>3+</sup> Nano-Glass-Ceramics Made from Sol – Gel Method at Low Temperature. *Nanomaterials* **2022**, *12*.
9. Fiume, E.; Cao, S.P.O.; Na, M.; Migneco, C.; Vern, E. On the Multicomponent. *Materials (Basel)*. **2020**, *13*.
10. Feng, S.; Qin, H.; Wu, G.; Jiang, H.; Zhao, J.; Liu, Y.; Luo, Z.; Qiao, J.; Jiang, J. Spectrum Regulation of YAG:Ce Transparent Ceramics with Pr, Cr Doping for White Light Emitting Diodes Application. *J. Eur. Ceram. Soc.* **2017**, doi:10.1016/j.jeurceramsoc.2017.03.061.
11. Wang, X.; Zhao, Z.; Wu, Q.; Li, Y.; Wang, Y. Synthesis, Structure and Photoluminescence Properties of Ca<sub>2</sub>LuHf<sub>2</sub>(AlO<sub>4</sub>)<sub>3</sub>:Ce<sup>3+</sup>, a Novel Garnet-Based Cyan Light-Emitting Phosphor. *J. Mater. Chem. C* **2016**, doi:10.1039/c6tc03933b.
12. Almessiere, M.A.; Ahmed, N.M.; Massoudi, I.; Al-Otaibi, A.L.; Al-shehri, A.A.; Shafouri, M. Al Study of the Structural and Luminescent Properties of Ce<sup>3+</sup> and Eu<sup>3+</sup> Co-Doped YAG Synthesized by Solid State Reaction. *Optik (Stuttg)*. **2018**, doi:10.1016/j.ijleo.2017.12.031.
13. Shmurak, S.Z.; Kiselev, A.P.; Kurmasheva, D.M.; Red'kin, B.S.; Sinitsyn, V. V. Effect of Solid-Phase Amorphization on the Spectral Characteristics of Europium-Doped Gadolinium Molybdate. *J. Exp. Theor. Phys.* **2010**, doi:10.1134/S1063776110050055.
14. Dai, Z.; Boiko, V.; Grzeszkiewicz, K.; Markowska, M.; Ursi, F.; Hölsä, J.; Saladino, M.L.; Hreniak, D. Effect of Annealing Temperature on Persistent Luminescence of Y<sub>3</sub>Al<sub>2</sub>Ga<sub>3</sub>O<sub>12</sub>:Cr<sup>3+</sup> Co-Doped with Ce<sup>3+</sup> and Pr<sup>3+</sup>. *Opt. Mater. (Amst)*. **2021**, doi:10.1016/j.optmat.2020.110522.
15. Shinde, V. V.; Tiwari, A.; Dhoble, S.J. Synthesis of RE<sup>3+</sup> (RE<sup>3+</sup> = Ce<sup>3+</sup>, Dy<sup>3+</sup>, Eu<sup>3+</sup> and Tb<sup>3+</sup>) Activated Gd<sub>2</sub>SiO<sub>5</sub> Optoelectronics Materials for Lighting. *J. Mol. Struct.* **2020**, doi:10.1016/j.molstruc.2020.128397.
16. Maćzka, M.; Bednarkiewicz, A.; Mendoza-Mendoza, E.; Fuentes, A.F.; Kępiński, L. Low-Temperature Synthesis, Phonon and Luminescence Properties of Eu Doped Y<sub>3</sub>Al<sub>5</sub>O<sub>12</sub> (YAG) Nanopowders. *Mater. Chem. Phys.* **2014**, *143*, 1039–1047, doi:10.1016/j.matchemphys.2013.11.002.
17. Pan, Y.; Wu, M.; Su, Q. Tailored Photoluminescence of YAG:Ce Phosphor through Various Methods. *J. Phys. Chem. Solids* **2004**, doi:10.1016/j.jpcs.2003.08.018.
18. Pankratov, V.; Shirmane, L.; Chudoba, T.; Gluchowski, P.; Hreniak, D.; Streck, W.; Lojkowski, W. Peculiarities of Luminescent Properties of Cerium Doped YAG Transparent Nanoceramics. *Radiat. Meas.* **2010**, *45*, 392–394, doi:10.1016/j.radmeas.2009.12.014.
19. Shirmane, L.; Pankratov, V. Emerging Blue-UV Luminescence in Cerium Doped YAG Nanocrystals. *Phys. Status Solidi - Rapid Res. Lett.* **2016**, *10*, 475–479, doi:10.1002/pssr.201600041.
20. Inkraite, G.; Zabiliute-Karaliune, A.; Aglinskaite, J.; Vitta, P.; Kristinaityte, K.; Marsalka, A.; Skaudzius, R. Study of YAG: Ce and Polymer Composite Properties for Application in LED Devices. *Chempluschem* **2020**, *85*, 1504–1510, doi:10.1002/cplu.202000318.
21. Kajihara, K. Recent Advances in Sol-Gel Synthesis of Monolithic Silica and Silica-Based Glasses. *J. Asian Ceram. Soc.* **2013**, *1*, 121–133, doi:10.1016/j.jascr.2013.04.002.

**Disclaimer/Publisher's Note:** The statements, opinions and data contained in all publications are solely those of the individual author(s) and contributor(s) and not of MDPI and/or the editor(s). MDPI and/or the editor(s) disclaim responsibility for any injury to people or property resulting from any ideas, methods, instructions or products referred to in the content.